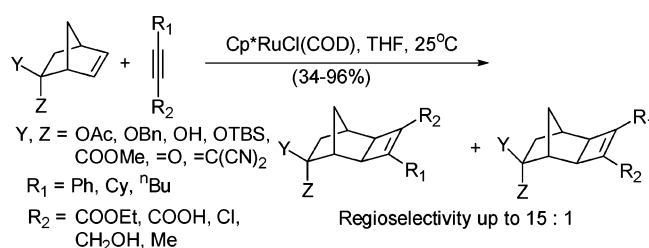


## Remote Substituent Effects in Ruthenium-Catalyzed [2+2] Cycloadditions: An Experimental and Theoretical Study

Peng Liu, Robert W. Jordan, Steven P. Kibbee, John D. Goddard,\* and William Tam\*  
*Guelph-Waterloo Centre for Graduate Work in Chemistry and Biochemistry, Department of Chemistry,  
 University of Guelph, Guelph, Ontario, Canada N1G 2W1*

wtam@uoguelph.ca; jgoddard@uoguelph.ca

Received January 18, 2006



The effects of a remote substituent on the regioselectivity of ruthenium-catalyzed [2+2] cycloadditions of 2-substituted norbornenes with alkynes have been investigated experimentally and theoretically using density functional theory. Most of the cycloadditions occurred smoothly at room temperature, giving the exo cycloadducts in excellent yields. Regioselectivities of 1.2:1 to 15:1 were observed with various substituents on the C-2 position of the norbornenes. Exo-C-2-substituents usually showed greater remote substituent effects on the regioselectivities of the cycloadditions than the corresponding endo-C-2-substituents. The regioselectivity of the cycloadditions with C-2 substituents containing an exocyclic double bond (sp<sup>2</sup> hybridized carbon at C-2) are much higher than the cycloadditions with the exo and endo 2-substituted norbornenes. Theoretical studies predicted the same trends as experiment and matched the experimental product ratios well. The nature of the regioselectivity in this reaction is discussed. Different strengths of the  $\pi(C^5-C^6) \rightarrow \pi^*(C^2-Y)$  or  $\pi(C^5-C^6) \rightarrow \sigma^*(C^2-Y)$  orbital interactions in 2-substituted norbornenes result in different degrees of C<sup>5</sup>-C<sup>6</sup> double bond polarization. Stronger C<sup>5</sup>-C<sup>6</sup> polarization will increase the difference in the activation energies between the major and minor pathways and thus lead to greater regioselectivities.

### Introduction

The study of remote electronic effects in controlling the regio- and stereoselectivities of nucleophilic and electrophilic additions to  $\pi$ -bonds has attracted considerable interest.<sup>1,2</sup> The most common systems for these studies are 7-oxabicyclo[2.2.1]hept-5-ene derivatives (**1**),<sup>3</sup> 7-norbornanones (**2**),<sup>4</sup> 7-methylenenorbornanes (**3**),<sup>5</sup> and 2-substituted norbornenes (**4**).<sup>6,7</sup> (Figure 1). We have recently studied the effect of a remote substituent on the regioselectivity of oxymercuration reactions of 2-substituted norbornenes (**4**).<sup>7b</sup> Moderate to high levels of regioselectivity were observed with both exo- and endo-substituents at C-2 of norbornenes (Scheme 1).

Unlike the remote substituent effects on nucleophilic and electrophilic additions that have been studied extensively, usually showing strong remote stereoelectronic effects in controlling the regio- and stereoselectivities, examples of remote substituent effects on transition-metal-catalyzed cycloadditions are very rare in the literature and usually only low levels of selectivities were observed.<sup>3f,7c,8</sup> For example, in the Co-catalyzed Pauson-Khand [2+2+1] cycloadditions of 2-substituted norbornenes, the C-2 remote substituents showed only very

(1) For recent reviews, see: (a) Cieplak, A. S. *Chem. Rev.* **1999**, *99*, 1265. (b) Ohwada, T. *Chem. Rev.* **1999**, *99*, 1337. (c) Mehta, G.; Chandrasekhar, J. *Chem. Rev.* **1999**, *99*, 1437.

(2) (a) Gung, B. W. *Tetrahedron* **1996**, *52*, 5263. (b) Fraser, R. R.; Faibish, N. C.; Kong, F.; Bednarski, J. *J. Org. Chem.* **1997**, *62*, 6167.

(3) (a) Black, K. A.; Vogel, P. *J. Org. Chem.* **1986**, *51*, 5341. (b) Arjona, O.; de la Pradilla, R. F.; Plumet, J.; Viso, A. *Tetrahedron* **1989**, *45*, 4565. (c) Arjona, O.; de la Pradilla, R. F.; Garcia, L.; Mallo, A.; Plumet, J. *J. Chem. Soc., Perkin Trans. 2* **1989**, 1315. (d) Arjona, O.; de la Pradilla, R. F.; Pita-Romero, I.; Plumet, J.; Viso, A. *Tetrahedron* **1990**, *46*, 8199. (e) Arjona, O.; Manzano, C.; Plumet, J. *Heterocycles* **1993**, *35*, 63. (f) Arjona, O.; Csáky, A. G.; Murcia, M. C.; Plumet, J. *J. Org. Chem.* **1999**, *64*, 7338. (g) Arjona, O.; Csáky, A. G.; Murcia, M. C.; Plumet, J. *J. Org. Chem.* **1999**, *64*, 9739.

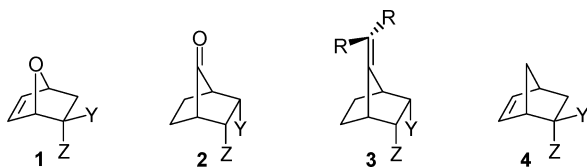
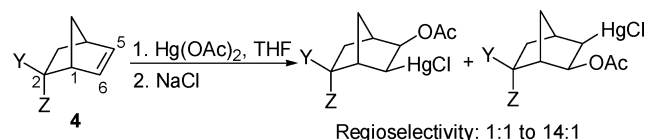
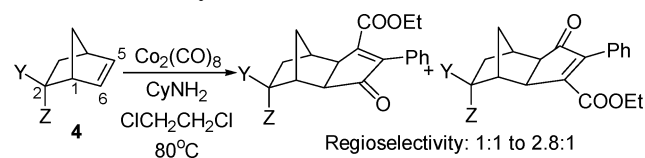


**FIGURE 1.** Study of remote substituent effects in different bicyclic systems.

**SCHEME 1. Remote Substituent Effects on Oxymercuration**



**SCHEME 2. Remote Substituent Effects on the Pauson–Khand Cycloaddition**



weak remote stereoelectronic effects and low levels of regioselectivities (1:1 to 2.8:1) were observed (Scheme 2).<sup>7c</sup> In this paper, we report our experimental and theoretical results on remote substituent effects in ruthenium-catalyzed [2+2] cycloadditions of 2-substituted norbornenes with unsymmetrical alkynes. To the best of our knowledge, no example of controlling regioselectivity of any metal-catalyzed [2+2] cycloadditions by a remote substituent has been reported in the literature prior to this study.

Quantum chemical methods have been widely used to study the mechanisms and selectivities of organic reactions. Recently, quantitative predictions of stereoselectivities have been applied to organic reactions, such as aldol reactions,<sup>9a</sup> 1,3-dipolar cycloadditions,<sup>9b</sup> alkylation reactions,<sup>9c</sup> and benzoin condensations.<sup>9d</sup> However, theoretical predictions of transition-metal-

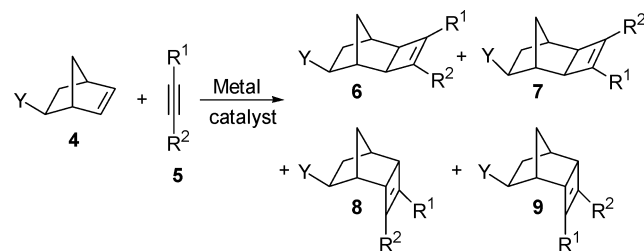
catalyzed reactions are much rarer because of the complexity of the reaction mechanisms and the higher computational cost of including the metal at reasonably high levels of theory and with adequate basis sets. The energy differences between different pathways are often less than a few kilocalories per mole in the reactions, and a suitable theoretical model is required to rationalize any computed energy differences. In this paper, we report the use of density functional methods both to explain qualitatively and to predict quantitatively the ratios of isomeric products of the ruthenium-catalyzed [2+2] cycloadditions of 2-substituted norbornenes and unsymmetrical alkynes.

Theoretical interpretations of the substituent effects have been proposed on the basis of stereoelectronic arguments in previous studies of regioselective reactions of 2-substituted norbornenes.<sup>7</sup> In this paper, in addition to the electrostatic analysis, we use a homoconjugation model and a theoretical picture of through-space orbital interactions to rationalize the remote substituent effects. The orbital interactions in norbornene and norbornadiene derivatives have been studied extensively to understand the  $\pi$  facial reactivities and selectivities.<sup>1b,4b,f,5b,10</sup> However, there are few previous studies which deal with the effects of remote substituents at the C-2 position that control the regioselectivity of reactions of the C<sup>5</sup>–C<sup>6</sup> double bond.<sup>6,7</sup> In this paper, we examine the orbital interactions which connect C-2 substituent effects to the polarization of the C<sup>5</sup>–C<sup>6</sup> double bond, the relative stability of the transition-state structures, and finally the regioselectivities.

**Results and Discussion**

**Remote Substituent Effects of Exo and Endo 2-Substituted Norbornenes on Ru-Catalyzed [2+2] Cycloadditions with Alkyne 5a.** Four different [2+2] cycloadducts are theoretically possible in the cycloaddition between a 2-substituted norbornene **4** and an unsymmetrical alkyne **5** (Scheme 3). On the basis of our previous work and others,<sup>11</sup> Cp\*RuCl(COD)-catalyzed [2+2] cycloadditions between bicyclic alkenes and alkynes usually produced only the exo cycloadducts. Thus, although four possible cycloadducts could be formed, we anticipated that only regioisomers of the exo cycloadducts, **6** and **7**, would be formed in the cycloadditions.

**SCHEME 3. Possible [2+2] Cycloadducts between a 2-Substituted Norbornene and an Unsymmetrical Alkyne**



When an equimolar amount of norbornene **4a** (Y = *exo*-OAc) and alkyne **5a** (R<sup>1</sup> = Ph, R<sup>2</sup> = COOEt) was treated with 5 mol % of Cp\*RuCl(COD) at 80 °C for 60 h without solvent, only

(4) (a) Mehta, G.; Khan, F. A. *J. Am. Chem. Soc.* **1990**, *112*, 6140. (b) Mehta, G.; Khan, F. A.; Ganguly, B.; Chandrasekhar, J. *J. Chem. Soc., Chem. Commun.* **1992**, 1711. (c) Ganguly, B.; Chandrasekhar, J.; Khan, F. A.; Mehta, G. *J. Org. Chem.* **1993**, *58*, 1734. (d) Mehta, G.; Khan, F. A. *J. Chem. Soc., Perkin Trans. 1* **1993**, 1727. (e) Mehta, G.; Khan, F. A.; Ganguly, B.; Chandrasekhar, J. *J. Chem. Soc., Perkin Trans. 2* **1994**, 2275. (f) Mehta, G.; Khan, F. A.; Adcock, W. *J. Chem. Soc., Perkin Trans. 2* **1995**, 2189. (g) Mehta, G.; Khan, F. A.; Mohal, N.; Narayan, I. N.; Kalyanaraman, P.; Chandrasekhar, J. *J. Chem. Soc., Perkin Trans. 1* **1996**, 2665. (h) Mehta, G.; Ravikrishna, C.; Kalyanaraman, P.; Chandrasekhar, J. *J. Chem. Soc., Perkin Trans. 1* **1998**, 1895. (i) Mehta, G.; Mohal, N. *J. Chem. Soc., Perkin Trans. 1* **1998**, 505.

(5) (a) Mehta, G.; Khan, F. A. *J. Chem. Soc., Chem. Commun.* **1991**, 18. (b) Mehta, G.; Khan, F. A.; Gadre, S. R.; Shirsat, R. N.; Ganguly, B.; Chandrasekhar, J. *Angew. Chem., Int. Ed. Engl.* **1994**, *33*, 1390. (c) Mehta, G.; Gunasekaran, G. *J. Org. Chem.* **1994**, *59*, 1953.

(6) (a) Arjona, O.; de la Pradilla, R. F.; Plumet, J.; Viso, A. *J. Org. Chem.* **1991**, *59*, 6227. (b) Brands, K. M. J.; Kende, A. S. *Tetrahedron Lett.* **1992**, *33*, 5887.

(7) (a) Mayo, P.; Poirier, M.; Rainey, J.; Tam, W. *Tetrahedron Lett.* **1999**, *40*, 7727. (b) Mayo, P.; Orlova, G.; Goddard, J. D.; Tam, W. *J. Org. Chem.* **2001**, *66*, 5182. (c) Mayo, P.; Hecnar, T.; Tam, W. *Tetrahedron* **2001**, *57*, 5931. (d) Mayo, P.; Tam, W. *Tetrahedron* **2001**, *57*, 5943. (e) Mayo, P.; Tam, W. *Tetrahedron* **2002**, *58*, 9513. (f) Mayo, P.; Tam, W. *Tetrahedron* **2002**, *58*, 9527.

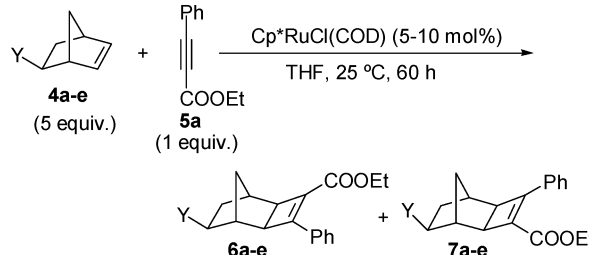
(8) (a) MacWhorter, S. E.; Sampath, V.; Olmstead, M. M.; Schore, N. E. *J. Org. Chem.* **1988**, *53*, 203. (b) Lautens, M.; Tam, W.; Edwards, L. E. *J. Chem. Soc., Perkin Trans. 1* **1994**, 2143.

(9) (a) Bahmanyar, S.; Houk, K. N.; Martin, H. J.; List, B. *J. Am. Chem. Soc.* **2003**, *125*, 2475. (b) Diaz, J.; Silva, M. A.; Goodman, J. M.; Pellegrinet, S. C. *Tetrahedron* **2005**, *61*, 10886. (c) Gordillo, R.; Carter, J.; Houk, K. N. *Adv. Synth. Catal.* **2004**, *346*, 1175. (d) Dudding, T.; Houk, K. N. *Proc. Natl. Acad. Sci. U.S.A.* **2004**, *101*, 5770.

(10) Mazzocchi, P. H.; Stahly, B.; Dodd, J.; Rondan, N. G.; Domelsmith, L. N.; Rozeboom, M. D.; Caramella, P.; Houk, K. N. *J. Am. Chem. Soc.* **1980**, *102*, 6482.

11% of a mixture of *exo* regioisomers **6a** and **7a** was obtained in a ratio of 3.1:1 (measured by GC and <sup>1</sup>H NMR). No *endo* isomers, **8** or **9**, were detected. Using hexanes, toluene, DMF, or 1,2-dichloroethane as solvent, low yields of the cycloadditions were observed (11–38%). However, with Et<sub>3</sub>N or THF as solvents, the yields increased considerably to 65 and 89%. Very small changes in the regioselectivities were observed with the use of different solvents. To optimize the yield and the regioselectivity of the cycloaddition, several reaction conditions were varied. Altering the equivalence of alkyne **5a** led to minimal changes in the regioselectivity. However, a dramatic reduction in the yield was observed as the equivalence of alkyne **5a** was increased. When 2 equiv of alkyne **5a** were used, the yield decreased to 29%, and when 5 equiv of alkyne **5a** were used, the yield was reduced to only 9%. On the other hand, increasing the number of equivalents of norbornene **4a** leads to higher yields and slightly greater regioselectivities. When 2 equiv of norbornene **4a** were used, the yield was 90% with regioselectivity increased to 4.2:1. When 5 equiv of norbornene **4a** were used, a quantitative yield was obtained with the same regioselectivity of 4.2:1. When we carried out the cycloadditions at different temperatures, we noticed that the cycloadditions occurred even at room temperature with essentially the same yield and regioselectivity. Thus, under optimized cycloaddition conditions, when 1 equiv of alkyne **5a** and 5 equiv of norbornene **4a** were treated with 5–10 mol % of Cp\**Ru*Cl(COD) in THF at room temperature, cycloadducts **6a** and **7a** were produced in 94% isolated yield in a ratio of 4.0:1 (Table 1, entry 1).

**TABLE 1.** Ruthenium-Catalyzed [2+2] Cycloadditions of Exo 2-Substituted Norbornenes



entry	norbornene	Y	yield (%) <sup>a</sup>	6/7 <sup>b</sup>
1	<b>4a</b>	OAc	94	4.0:1
2	<b>4b</b>	OBn	93	3.0:1
3	<b>4c</b>	OTBS	92	1.5:1
4	<b>4d</b>	OH	91	2.0:1
5	<b>4e</b>	COOMe	96	2.4:1

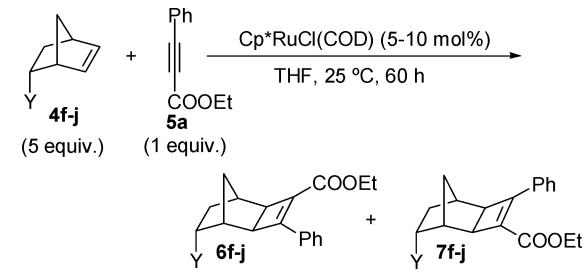
<sup>a</sup> Isolated yields after column chromatography. <sup>b</sup> Ratios measured by GC and/or by <sup>1</sup>H NMR and based on the average number from two to four runs.

To study the effect of the remote Y substituent of norbornene **4** on the cycloaddition, *exo* and *endo* 2-substituted norbornenes

(11) For ruthenium-catalyzed [2+2] cycloadditions, see: (a) Mitsudo, T.; Naruse, H.; Kondo, T.; Ozaki, Y.; Watanabe, Y. *Angew. Chem., Int. Ed. Engl.* **1994**, *33*, 580. (b) Jordan, R. W.; Tam, W. *Org. Lett.* **2000**, *2*, 3031. (c) Jordan, R. W.; Tam, W. *Org. Lett.* **2001**, *3*, 2367. (d) Jordan, R. W.; Tam, W. *Tetrahedron Lett.* **2002**, *43*, 6051. (e) Villeneuve, K.; Jordan, R. W.; Tam, W. *Synlett* **2003**, 2123. (f) Villeneuve, K.; Tam, W. *Angew. Chem., Int. Ed.* **2004**, *43*, 610. (g) Jordan, R. W.; Khoury, P. K.; Goddard, J. D.; Tam, W. *J. Org. Chem.* **2004**, *69*, 8467. (h) Villeneuve, K.; Riddell, N.; Jordan, R. W.; Tsui, G. C.; Tam, W. *Org. Lett.* **2004**, *6*, 4543. (i) Riddell, N.; Villeneuve, K.; Tam, W. *Org. Lett.* **2005**, *7*, 3681. (j) Mitsudo, T.; Kokuryo, K.; Takegami, Y. *J. Chem. Soc., Chem. Commun.* **1976**, 772. (k) Mitsudo, T.; Kokuryo, K.; Shinsugi, T.; Nakagawa, Y.; Watanabe, Y.; Takegami, Y. *J. Org. Chem.* **1979**, *44*, 4492.

**4a–j** (Y = COOMe, OH, OTBS, OBn, OAc) were prepared<sup>7e</sup> and their ruthenium-catalyzed [2+2] cycloadditions with alkyne **5a** were studied (Tables 1 and 2). Under optimized reaction conditions, both *exo*- and *endo*-norbornenes undergo ruthenium-catalyzed [2+2] cycloadditions with alkyne **5a** smoothly, giving the corresponding cycloadducts in excellent yields. The regioselectivities were only modest, and generally, *exo*-norbornenes gave higher regioselectivities than their corresponding *endo* isomers. For *exo*-norbornenes **4a–e**, regioselectivities of 1.5:1 to 4.0:1 were observed, with **4a** (Y = OAc) giving the highest regioselectivity. In the case of *endo*-norbornenes **4f–j**, very little difference in regioselectivities was observed with different Y substituents.

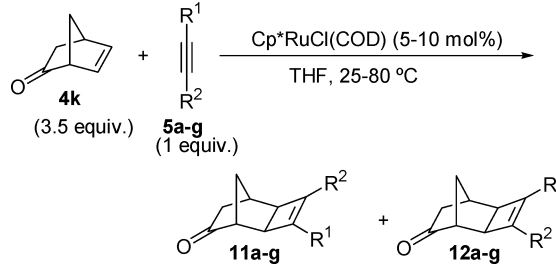
**TABLE 2.** Ruthenium-Catalyzed [2+2] Cycloadditions of Endo 2-Substituted Norbornenes



entry	norbornene	Y	yield (%) <sup>a</sup>	6/7 <sup>b</sup>
1	<b>4f</b>	OAc	94	1.4:1
2	<b>4g</b>	OBn	92	1.2:1
3	<b>4h</b>	OTBS	93	2.0:1
4	<b>4i</b>	OH	90	1.4:1
5	<b>4j</b>	COOMe	91	2.0:1

<sup>a</sup> Isolated yields after column chromatography. <sup>b</sup> Ratios measured by GC and/or by <sup>1</sup>H NMR and based on the average number from two to four runs.

**Remote Substituent Effects of 2-Substituted Norbornenes with the C-2 Substituent Containing an Exocyclic Double Bond (sp<sup>2</sup>-Hybridized Carbon at C-2) in Ru-Catalyzed [2+2] Cycloadditions with Alkynes 5a–g.** During our studies on the remote substituent effects on the cobalt-catalyzed Pauson–Khand [2+2+1] cycloadditions of 2-substituted norbornenes,<sup>7d</sup> although the C-2 remote substituents only showed very weak remote stereoelectronic effects and low levels of regioselectivities (1:1 to 2.8:1) were observed, the highest regioselectivity was observed with 2-norbornenone **4k**, with a sp<sup>2</sup>-hybridized carbon at C-2. When 2-norbornenone **4k** was subjected to the Ru-catalyzed cycloaddition conditions with alkyne **5a**, an excellent yield (96%) and a better regioselectivity (7.5:1) were observed (Table 3, entry 1; compare with Tables 1 and 2). We then studied the ruthenium-catalyzed [2+2] cycloadditions of 2-norbornenone **4k** with several different alkynes, and the results are shown in Table 3. When an ester moiety is attached to the acetylenic carbon (R<sup>2</sup> = COOEt, **5a–c**, entries 1–3), the Ru-catalyzed cycloadditions occurred smoothly at room temperature giving excellent yields of the [2+2] cycloadducts and the regioselectivity improved from 7.5:1 (when R<sup>1</sup> = Ph) to 8.2:1 (R<sup>1</sup> = <sup>n</sup>Bu); the highest regioselectivity of 10:1 was observed when R<sup>1</sup> = Cy (cyclohexyl). Comparing the alkynes with a Ph group attached to the acetylenic carbon (entries 1 and 4–7), alkynes with ester (**5a**, R<sup>2</sup> = COOEt) and carboxylic acid (**5d**, R<sup>2</sup> = COOH) moieties gave excellent yields in the cycloadditions at room temperature, whereas alkynes **5e–g** (with R<sup>2</sup> = Cl, CH<sub>2</sub>OH, and Me) required a higher reaction temperature

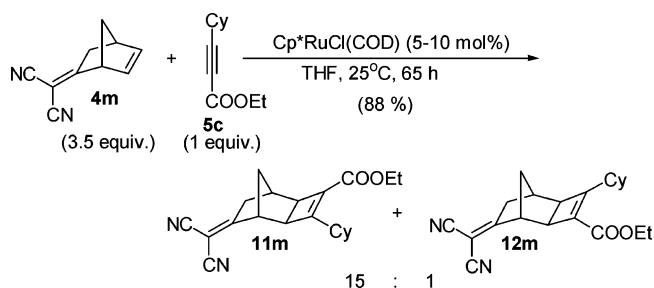
**TABLE 3.** Ruthenium-Catalyzed [2+2] Cycloadditions of 2-Norbornenone **4k** with Different Alkynes


entry <sup>a</sup>	alkyne	R <sup>1</sup>	R <sup>2</sup>	yield (%) <sup>b</sup>	11/12 <sup>c</sup>
1	<b>5a</b>	Ph	COOEt	96	7.5:1
2	<b>5b</b>	<sup>n</sup> Bu	COOEt	94	8.2:1
3	<b>5c</b>	Cy	COOEt	96	10:1
4	<b>5d</b>	Ph	COOH	95	7.9:1
5	<b>5e</b>	Ph	Cl	34 <sup>d</sup>	2.7:1
6	<b>5f</b>	Ph	CH <sub>2</sub> OH	63 <sup>d</sup>	1.6:1
7	<b>5g</b>	Ph	Me	95	1.4:1

<sup>a</sup> For entries 1–4, the reactions were run at 25 °C for 45–70 h; for entries 5–7, the reactions were run at 60–80 °C for 115–165 h. <sup>b</sup> Isolated yields after column chromatography. <sup>c</sup> Ratios measured by GC and/or by <sup>1</sup>H NMR and based on the average number from two to four runs. <sup>d</sup> Incomplete reaction; unreacted alkyne was recovered.

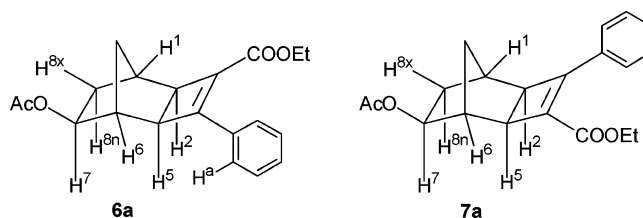
(60–80 °C). Although alkyne **5g** (R<sup>2</sup> = Me) gave an excellent yield in the cycloaddition, alkynes **5e** and **5f** are both less reactive and the cycloadditions were incomplete after stirring at 80 °C for 165 h. Comparing the regioselectivities of these Ph-substituted alkynes (**5a** and **5d–g**), we observed good and similar regioselectivities for **5a** (R<sup>2</sup> = COOEt, 7.5:1) and **5d** (R<sup>2</sup> = COOH, 7.9:1) but low levels of regioselectivities were observed with **5e** (R<sup>2</sup> = Cl, 2.7:1), **5f** (R<sup>2</sup> = CH<sub>2</sub>OH, 1.6:1), and **5g** (R<sup>2</sup> = Me, 1.4:1).

To determine if other 2-substituted norbornenes, with the C-2 substituent being an exocyclic double bond (sp<sup>2</sup>-hybridized carbon at C-2), also give higher regioselectivity in the Ru-catalyzed cycloaddition than exo and endo 2-substituted norbornenes **4a–j**, as in 2-norbornenone **5k**, we have synthesized norbornene **4m**<sup>12</sup> and studied its Ru-catalyzed cycloaddition with alkyne **5c** (Scheme 4). To our delight, similar to 2-norbornenone **4k**, the Ru-catalyzed cycloaddition between 2-norbornene **4m** and alkyne **5c** occurred smoothly at room temperature, giving the cycloadducts in good yield and an excellent regioselectivity of 15:1. Thus, the dicyanomethylene group gave the strongest remote stereoelectronic effects in the Ru-catalyzed cycloaddition.

**SCHEME 4.** Ruthenium-Catalyzed [2+2] Cycloadditions of Norbornene **4m** with Alkyne **5c**

**Determination of Regio- and Stereochemistry of the Cycloadducts.** The exo and endo stereochemistry of the

cycloadducts can easily be distinguished by the coupling constants of H<sup>2</sup> and H<sup>5</sup> (Figure 2 and Scheme 3) in the <sup>1</sup>H NMR.<sup>13</sup> Several exo and endo cycloadducts were modeled for energy minimization at the PM3 level (CS Chem 3D Pro, Version 3.5.1) using MOPAC for the assessment of the dihedral angles between H<sup>2</sup> and H<sup>5</sup>. These dihedral angles were then compared to the Karplus curve for the determination of the theoretical coupling constants. On the basis of these computational studies, the dihedral angles between H<sup>5</sup> and H<sup>6</sup> (or between H<sup>1</sup> and H<sup>2</sup>) in the exo cycloadducts **6** and **7** (Scheme 3 and Figure 2) are in the range of 70°–75°; the coupling constant between H<sup>5</sup> and H<sup>6</sup> (or between H<sup>1</sup> and H<sup>2</sup>) would be very small (*J* ~ 0–2 Hz). On the other hand, in the endo cycloadducts **8** and **9**, the dihedral angles between H<sup>5</sup> and H<sup>6</sup> (or between H<sup>1</sup> and H<sup>2</sup>) are in the range of 35°–40° and would give a coupling constant of 6–9 Hz between H<sup>5</sup> and H<sup>6</sup> (or between H<sup>1</sup> and H<sup>2</sup>). In all the cycloadducts that we obtained, the coupling constants between H<sup>5</sup> and H<sup>6</sup> (or between H<sup>1</sup> and H<sup>2</sup>) are always less than 1 Hz, and therefore, all the cycloadducts must have exo stereochemistry.

**FIGURE 2.** Determination of regio- and stereochemistry of the cycloadducts.

For the cycloadducts **6a** (*exo*-OAc, Table 1), **6f** (*endo*-OAc, Table 2), **6j** (*endo*-COOMe, Table 2), **11a** and **11c** (ketone group, Table 3), and **11m** (dicyanomethylene group, Scheme 4), we were able to isolate and separate the major regioisomers from the mixture of regioisomers in the cycloadditions either by fractional recrystallization or by column chromatography. To determine the regiochemistry of the cycloadducts unambiguously by using several NMR techniques (HCOSY, HSQC, HMBC, and NOESY or GOESY experiments).<sup>14,15</sup> To distinguish the two regioisomers **6a** and **7a** (Figure 2), NOESY or GOESY experiments were used. In the GOESY experiments of the major regioisomer (**6a**), H<sup>5</sup> (at 2.79 ppm) showed +ve NOE with H<sup>2</sup> (2.64 ppm), H<sup>7</sup> (4.63 ppm), H<sup>6</sup> (2.35 ppm), and H<sup>a</sup> (Ar–H, at 8.02 ppm); H<sup>2</sup> (at 2.64 ppm) in **6a** showed a +ve NOE effect with H<sup>5</sup> (2.79 ppm), H<sup>1</sup> (2.33 ppm), and H<sup>8a</sup> (1.73

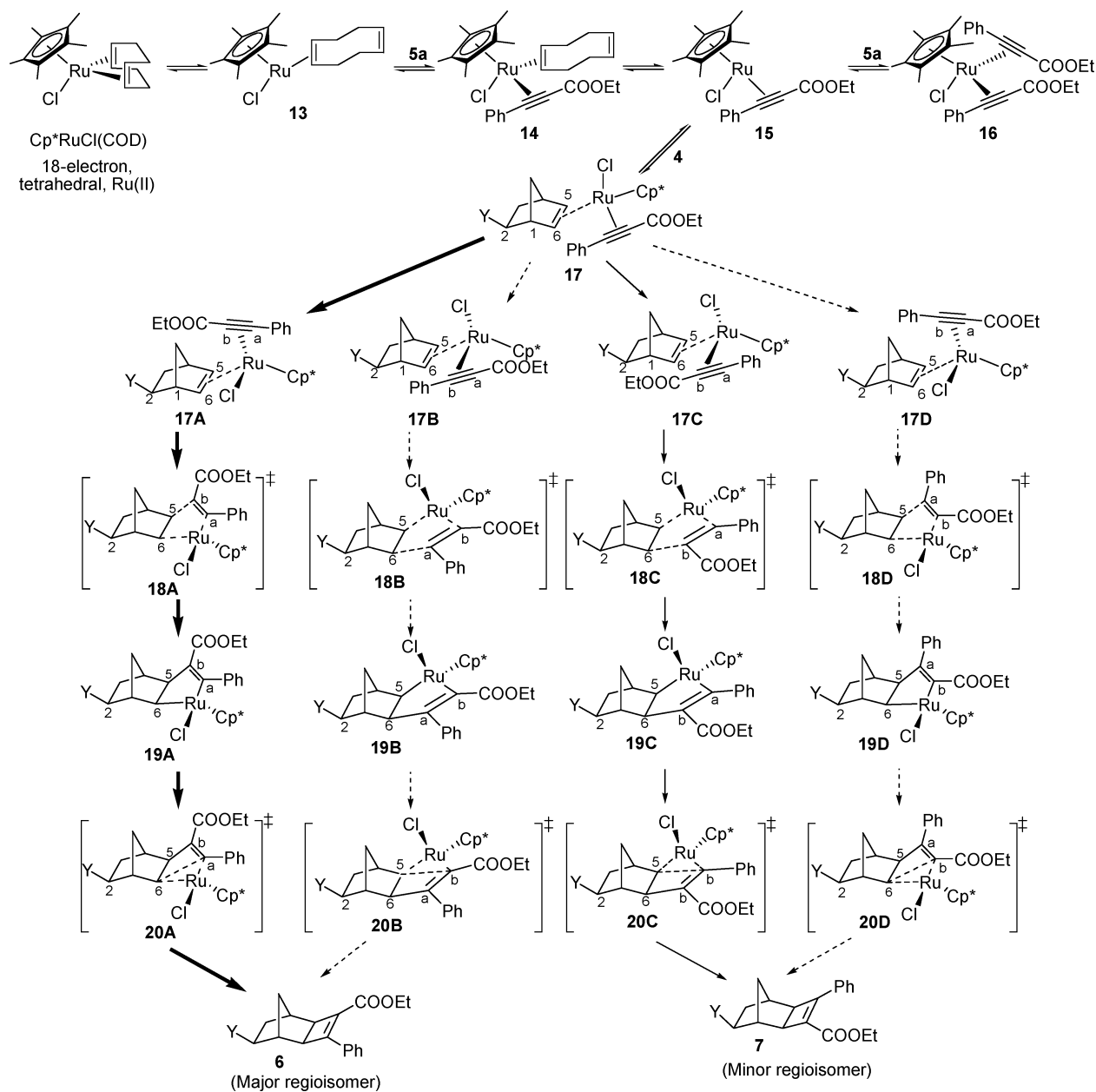
(13) Similar methods have been used for the assignment of exo and endo stereochemistries of bicyclic alkanes and alkenes. See: (a) Yip, C.; Handerson, S.; Jordan, R.; Tam, W. *Org. Lett.* **1999**, *1*, 791. (b) Tranmer, G. K.; Keech, P.; Tam, W. *Chem. Commun.* **2000**, 863. (c) Yip, C.; Handerson, S.; Tranmer, G. K.; Tam, W. *J. Org. Chem.* **2001**, *66*, 276. (d) Tranmer, G. K.; Tam, W. *J. Org. Chem.* **2001**, *66*, 5113. (e) Flautt, T. J.; Erman, W. F. *J. Am. Chem. Soc.* **1963**, *85*, 3212. (f) Meinwald, J.; Meinwald, Y. C.; Baker, T. N., III. *J. Am. Chem. Soc.* **1964**, *86*, 4074. (g) Smith, C. D. *J. Am. Chem. Soc.* **1966**, *88*, 4273. See also: refs 11a–k.

(14) HCOSY: <sup>1</sup>H–<sup>1</sup>H correlated spectroscopy. HSQC: heteronuclear single quantum coherence. HMBC: heteronuclear multiple bond correlation. NOESY: nuclear overhauser enhancement spectroscopy. See: Crews, P.; Rodriguez, J.; Jaspars, M. *Organic Structure Analysis*; Oxford University Press: Oxford, 1998.

(15) GOESY: gradient enhanced nuclear Overhauser enhancement spectroscopy. See: (a) Stonehouse, J.; Adell, P.; Keeler, J.; Shaka, A. J. *J. Am. Chem. Soc.* **1994**, *116*, 6037. (b) Stott, K.; Stonehouse, J.; Keeler, J.; Hwang, T.-L.; Shaka, A. J. *J. Am. Chem. Soc.* **1995**, *117*, 4199. (c) Dixon, A. M.; Widmalm, G.; Bull, T. E. *J. Magn. Reson.* **2000**, *147*, 266.

(12) Carrupt, P. A.; Vogel, P. *Helv. Chim. Acta* **1989**, *72*, 1008.

## SCHEME 5. Proposed Mechanism



ppm), but no NOE was observed with any Ar-H ( $H^a$ ). Similar methods were used to determine the regiochemistry of most of the cycloadducts (both major and minor isomers). Cycloadducts for which we had difficulty in assigning the regiochemistry by the above NMR techniques were chemically converted to cycloadducts with known regiochemistries, and their NMR spectra were compared. In all cases, all the major regioisomers were found to have similar regiochemistry, having the C-2 remote substituent “syn” to the Ph group and “anti” to the COOEt group (as in **6a**, Figure 2). These assignments also were supported by X-ray crystallography.<sup>16</sup>

(16) X-ray structures of the major regioisomers of the cycloadducts **6a**, **6j**, **11a**, and **11m** were obtained, and their structures were reported: (a) Schlaf, M.; Jordan, R. W.; Tam, W. *Acta Crystallogr.* **2002**, *E58*, o629. (b) Lough, A. J.; Jordan, R. W.; Tam, W. *Acta Crystallogr.* **2003**, *E59*, o1675. (c) Tam, W.; Lough, A. J.; Jordan, R. W. *Acta Crystallogr.* **2003**, *E59*, o1685. (d) Jordan, R. W.; Tam, W.; Lough, A. J. *Acta Crystallogr.* **2003**, *E59*, o1687.

**Discussion of the Mechanism.** Previous studies have shown that formation of a cationic  $[Cp^*Ru]^+$  species from  $Cp^*RuCl(COD)$  by treatment with  $AgOTf$  decreased the catalytic activity, and low yields (<25%) of the cycloadducts were observed.<sup>11</sup> This result suggested that a neutral  $[Cp^*RuCl]$  moiety is likely to be the active catalytic species in the cycloadditions. A proposed mechanism of the Ru-catalyzed [2+2] cycloadditions between 2-substituted norbornenes **4** and alkyne **5a** is shown in Scheme 5.

Dissociation of one of the double bonds of the cyclooctadiene (COD) ligand from the catalyst  $Cp^*RuCl(COD)$  followed by ligand association with alkyne **5a** will provide complex **14** (Scheme 5). Upon dissociation of the COD ligand to form the coordinatively unsaturated complex **15**, either another molecule of alkyne **5a** or 2-substituted norbornene **4** could complex with **15**. In the studies of the effect of the number of equivalents of norbornene **4a** and alkyne **5a**, we noticed that the use of an

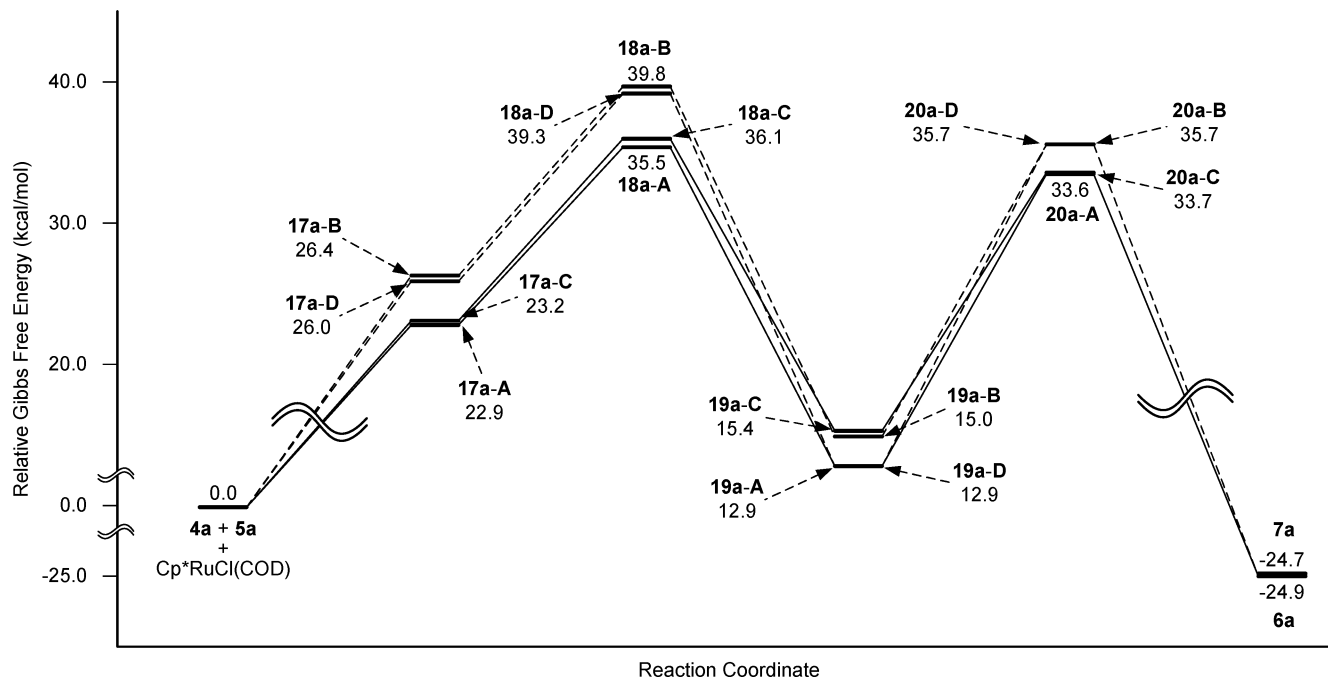


**FIGURE 3.** Potential energy profile of the solvent-free model for Ru-catalyzed [2+2] cycloaddition between norbornene **4a** ( $Y = \text{exo-OAc}$ ) and alkyne **5a** ( $R^1 = \text{Ph}$ ,  $R^2 = \text{COOEt}$ ). Energies are Gibbs free energies in kcal/mol, with respect to separated reactants **4a** + **5a** +  $\text{Cp}^*\text{RuCl}(\text{COD})$ .

excess of the alkene component improves the yields of the cycloadditions but, on the other hand, the use of excess alkyne decreases the yield dramatically. When an excess of alkyne **5a** was used, complex **16** would form preferentially. Because Ru is known to form stronger  $\pi$ -complexes with alkynes than with alkenes,<sup>17</sup> the formation of complex **16** inhibits the cycloadditions. This explains why the use of an excess of the alkyne leads to low yields in the cycloadditions. When an excess of 2-substituted norbornene **4** was used, complexation of **15** to the  $\pi$  bond on the exo face of 2-substituted norbornene **4** would give complex **17**. In complex **17**, there are several ways that the four different groups (Cl,  $\text{Cp}^*$ , alkene **4**, and alkyne **5a**) attached to Ru can be arranged. On the basis of our theoretical studies in Ru-catalyzed [2+2] cycloadditions between bicyclic alkenes and alkynes,<sup>9g</sup> the most favorable arrangement (with the lowest energy) is with the Cl and the alkyne located above  $\text{C}^5$  and  $\text{C}^6$  and the  $\text{Cp}^*$  pointing away from the bicyclic alkene. Because both the bicyclic alkene (2-substituted norbornene **4**) and the alkyne (**5a**) are unsymmetrical, four different Ru-alkene-alkyne  $\pi$  complexes are possible (**17A–D**). The Cl can be located above  $\text{C}^6$  (syn to the  $\text{C}^2$  substituent, Y), and the alkyne can be located above  $\text{C}^5$ , as in **17A** and **17D**. In **17A**, the ester COOEt group of the unsymmetrical alkyne is pointing toward the bicyclic alkene and the Ph group of the alkyne is pointing away from the bicyclic alkene. On the other hand, the Cl can be located above  $\text{C}^5$  (anti to the  $\text{C}^2$  Y substituent) and the alkyne can be located above  $\text{C}^6$ , as in **17B** and **17C**. Oxidative addition of these Ru-alkene-alkyne  $\pi$  complexes **17A–D** would provide the metallacyclopentenes **19A–D**. Reductive elimination of both the metallacyclopentenes **19A** and **19B** would give

the major regioisomer **6**, whereas reductive elimination of the metallacyclopentenes **19C** and **19D** would give the minor regioisomer **7**.

**Theoretical Studies.** To gain further understanding of remote substituent effects on the regioselectivities in the cycloadditions between 2-substituted norbornenes and alkynes, a density functional study was performed. We studied the reactions of five different norbornenes, **4a** ( $Y = \text{exo-OAc}$ ), **4d** ( $Y = \text{exo-OH}$ ), **4f** ( $Y = \text{endo-OAc}$ ), **4i** ( $Y = \text{endo-OH}$ ), and **4k** ( $Y = \text{O}$ ), with alkyne **5a** ( $R^1 = \text{Ph}$ ,  $R^2 = \text{COOEt}$ ). Structures of the  $\pi$  complexes **17**, oxidative addition transition states **18**, metallacyclopentenes **19**, reductive elimination transition states **20**, and products **6** and **7** for all four possible pathways **A–D** were studied. The predicted potential energy profiles of the reaction between norbornene **4a** and alkyne **5a** are shown in Figure 3.

For all four pathways, the oxidative addition transition states **18a** have energies 2–4 kcal/mol higher than the reductive elimination transition states **20a**. This indicates that the oxidative addition is rate-determining for the overall reaction. The initial  $\pi$  complexes **17a** in pathways **A** and **C** are ca. 3 kcal/mol more stable than those in pathways **B** and **D**. The oxidative addition transition states **18a** in pathways **A** and **C** are ca. 4 kcal/mol more stable than those in pathways **B** and **D**. With the oxidative addition determining the rate, pathways **A** and **C** are preferred leading to products **6a** and **7a**, respectively. The oxidative addition transition state **18a-A** is 0.6 kcal/mol more stable than **18a-C**. This small energy difference in the rate-determining step could explain the very moderate product regioselectivity. The metallacyclopentenes **19a-A** and **19a-D** are ca. 2 kcal/mol more stable than **19a-B** and **19a-C**. The reductive elimination transition states **20a-A** and **20a-C** are ca. 2 kcal/mol more stable than **20a-B** and **20a-D**. The major product **6a** is 0.2 kcal/mol more stable than the minor product **7a**.

The potential energy profiles for the other four reactions are given in the Supporting Information. For all five reactions, the oxidative addition transition states **18** have higher energies than

(17) (a) Naota, T.; Takaya, H.; Murahashi, S.-I. *Chem. Rev.* **1998**, *98*, 2599. (b) Trost, B. M.; Toste, F. D.; Pinkerton, A. B. *Chem. Rev.* **2001**, *101*, 2067.

**TABLE 4.** Relative Free Energies (in kcal/mol) at 298 K for the Oxidative Addition Transition States **18** with Respect to the Separated Reactants

entry	norbornene	Y	alkyne	R <sup>1</sup>	R <sup>2</sup>	free energies, $\Delta G^{\ddagger}_{298(\text{theory})}$				$\Delta\Delta G^{\ddagger}_{298(\text{theory})}^a$ (calcd selectivity)	$\Delta\Delta G^{\ddagger}_{298(\text{exptl})}$ (exptl selectivity)
						<b>18-A</b>	<b>18-B</b>	<b>18-C</b>	<b>18-D</b>		
1	<b>4f</b>	endo-OAc	<b>5a</b>	Ph	COOEt	35.0	38.8	35.6	39.3	0.6 (2.8:1)	0.20 (1.4:1)
2	<b>4i</b>	endo-OH	<b>5a</b>	Ph	COOEt	32.0	36.9	32.4	37.3	0.4 (2.0:1)	0.20 (1.4:1)
3	<b>4d</b>	exo-OH	<b>5a</b>	Ph	COOEt	32.5	37.7	33.5	37.7	1.0 (5.4:1)	0.41 (2.0:1)
4	<b>4a</b>	exo-OAc	<b>5a</b>	Ph	COOEt	35.5	39.8	36.1	39.3	0.6 (2.8:1)	0.82 (4.0:1)
5	<b>4k</b>	O	<b>5a</b>	Ph	COOEt	32.9	38.4	34.2	36.8	1.3 (9.0:1)	1.19 (7.5:1)
6	<b>4k</b>	O	<b>5b</b>	<sup>n</sup> Bu	COOEt	29.6	35.7	31.1	35.7	1.5 (12:1)	1.24 (8.2:1)
7	<b>4k</b>	O	<b>5c</b>	Cy	COOEt	33.2	37.7	34.9	37.4	1.7 (18:1)	1.36 (10:1)
8	<b>4m</b>	C(CN) <sub>2</sub>	<b>5c</b>	Cy	COOEt	34.7	39.9	35.5	40.0	0.8 (3.9:1)	1.60 (15:1)

<sup>a</sup> Energy differences between preferred structures **18-A** and **18-C**.

**TABLE 5.** Relative Free Energies (in kcal/mol) in THF Solution at 298 K for the Oxidative Addition Transition States **18** with Respect to the Separated Reactants

entry	norbornene	Y	alkyne	R <sup>1</sup>	R <sup>2</sup>	free energies in THF, $\Delta G^{\ddagger}_{298(\text{THF, theory})}$				$\Delta\Delta G^{\ddagger}_{298(\text{THF, theory})}$ (exptl selectivity)	$\Delta\Delta G^{\ddagger}_{298(\text{exptl})}$ (exptl selectivity)
						<b>18-A</b>	<b>18-B</b>	<b>18-C</b>	<b>18-D</b>		
1	<b>4f</b>	endo-OAc	<b>5a</b>	Ph	COOEt	30.0	32.8	30.2	33.1	0.2 <sup>a</sup> (1.4:1)	0.20 (1.4:1)
2	<b>4i</b>	endo-OH	<b>5a</b>	Ph	COOEt	26.0	29.2	26.6	29.5	0.6 <sup>a</sup> (2.8:1)	0.20 (1.4:1)
3	<b>4d</b>	exo-OH	<b>5a</b>	Ph	COOEt	26.6	30.1	27.0	29.7	0.4 <sup>a</sup> (2.0:1)	0.41 (2.0:1)
4	<b>4a</b>	exo-OAc	<b>5a</b>	Ph	COOEt	29.2	33.6	30.6	32.9	1.4 <sup>a</sup> (11:1)	0.82 (4.0:1)
5	<b>4k</b>	O	<b>5a</b>	Ph	COOEt	26.3	30.6	28.0	30.1	1.7 <sup>a</sup> (18:1)	1.19 (7.5:1)
6	<b>4k</b>	O	<b>5b</b>	<sup>n</sup> Bu	COOEt	25.5	28.9	26.5	28.5	1.0 <sup>a</sup> (5.4:1)	1.24 (8.2:1)
7	<b>4k</b>	O	<b>5c</b>	Cy	COOEt	29.6	32.8	32.2	30.9	1.3 <sup>b</sup> (9.0:1)	1.36 (10:1)
8	<b>4m</b>	C(CN) <sub>2</sub>	<b>5c</b>	Cy	COOEt	33.2	36.9	36.2	34.8	1.6 <sup>b</sup> (15:1)	1.60 (15:1)

<sup>a</sup> Energy differences between preferred structures **18-A** and **18-C**. <sup>b</sup> Energy differences between preferred structures **18-A** and **18-D**.

the reductive elimination transition states **20**. The oxidative additions are rate-determining.

For greater completeness and reliability, we studied three more reactions: 2-norbornenone **4k** with alkynes **5b** (R<sup>1</sup> = <sup>n</sup>Bu, R<sup>2</sup> = COOEt) and with **5c** (R<sup>1</sup> = Cy, R<sup>2</sup> = COOEt) and norbornene **4m** (Y = C(CN)<sub>2</sub>) with alkyne **5c**. Because the theoretical results discussed above showed the oxidative addition steps to be rate-determining and to control regioselectivities, only the reactants and oxidative addition transition states **18** were studied for these three reactions. For all eight reactions, the relative Gibbs free energies at 298 K,  $\Delta G^{\ddagger}_{298(\text{theory})}$ , for the oxidative addition transition states **18-A–D** with respect to the separated reactants (norbornene, alkyne, and Cp<sup>\*</sup>RuCl(COD)) are given in Table 4. For all the reactions, the **18-A** transition states are more stable than **18-B**, and the **18-C** transition structures are more stable than **18-D**. Thus, pathway **A** is preferred leading to product **6**, and pathway **C** is preferred leading to product **7**. The energy differences between the two preferred oxidative addition transition states **18-A** and **18-C**,  $\Delta\Delta G^{\ddagger}_{298(\text{theory})}$ , control the product regioselectivity. The theoretically predicted regioselectivities and experimental activation free energy differences,  $\Delta\Delta G^{\ddagger}_{298(\text{exptl})}$ , are calculated using absolute rate theory:  $\ln(k_1/k_2) = -\Delta\Delta G^{\ddagger}/RT$ . These two sets of energy differences,  $\Delta\Delta G^{\ddagger}_{298(\text{theory})}$  and  $\Delta\Delta G^{\ddagger}_{298(\text{exptl})}$ , are given in Table 4. The theoretically predicted activation energy differences are in good agreement with the experimental free-energy differences derived from the product ratios. The mean absolute error between  $\Delta\Delta G^{\ddagger}_{298(\text{theory})}$  and  $\Delta\Delta G^{\ddagger}_{298(\text{exptl})}$  is 0.36 kcal/mol. Entries 3 and 8 have the greatest absolute errors of 0.6 and 0.8 kcal/mol, respectively. The experimental trends in regioselectivity could be explained well by these theoretical predictions (except for entries 3 and 8; see Table 5 for improvement to these exceptions when solvation effects are included). First, for all reactions, the transition states **18-A** are slightly more stable than **18-C**. Thus, pathway **A** is

predicted to be slightly favored, which means that the regioisomers **6** with a C<sup>2</sup> substituent anti to the electron-withdrawing group COOEt are always the major products. Second, in the experiments, norbornenes with exo-substituents (Table 4, entries 3 and 4) usually have higher selectivities than those with endo-substituents (Table 4, entries 1 and 2). The theoretically predicted activation energy differences of the norbornenes with the exo-substituents are greater (Y = OH) or equal (Y = OAc) to those with the endo-substituents. Third, except for entry 8 which has a slightly smaller activation energy difference than entry 3, the regioselectivities of the cycloadditions of norbornenes with C<sup>2</sup> substituents containing an exocyclic double bond (Table 4, entries 5–8) are predicted to be higher than those with the exo and endo 2-substituted norbornenes (Table 4, entries 1–4).

To include solvation effects in these studies, free energies in THF solution at 298 K of the reactants, products, and transition states were calculated with the PCM solvation model.<sup>18</sup> The potential energy profile of the reaction between norbornene **4a** and alkyne **5a** with the PCM model is shown in Figure 4. Results with this solvation model again indicate that the oxidative addition transition states **18a** have higher energies than the reductive elimination transition states **20a**. The oxidative addition again is predicted to be the rate-determining step, as in the gas-phase results. Free energies in THF solution  $\Delta G^{\ddagger}_{298(\text{THF, theory})}$  for the oxidative addition transition states **18** of the different reactions and pathways and the free-energy differences between the preferred pathways leading to the two regioisomers,  $\Delta\Delta G^{\ddagger}_{298(\text{THF, theory})}$ , are given in Table 5. It should be noted that, in entries 7 and 8, pathways **D** instead of pathways

(18) (a) Miertus, S.; Scrocco, E.; Tomasi, J. *Chem. Phys.* **1981**, *55*, 117. (b) Miertus, S.; Tomasi, J. *Chem. Phys.* **1982**, *65*, 239. (c) Cossi, M.; Barone, V.; Cammi, R.; Tomasi, J. *Chem. Phys. Lett.* **1996**, *255*, 327.

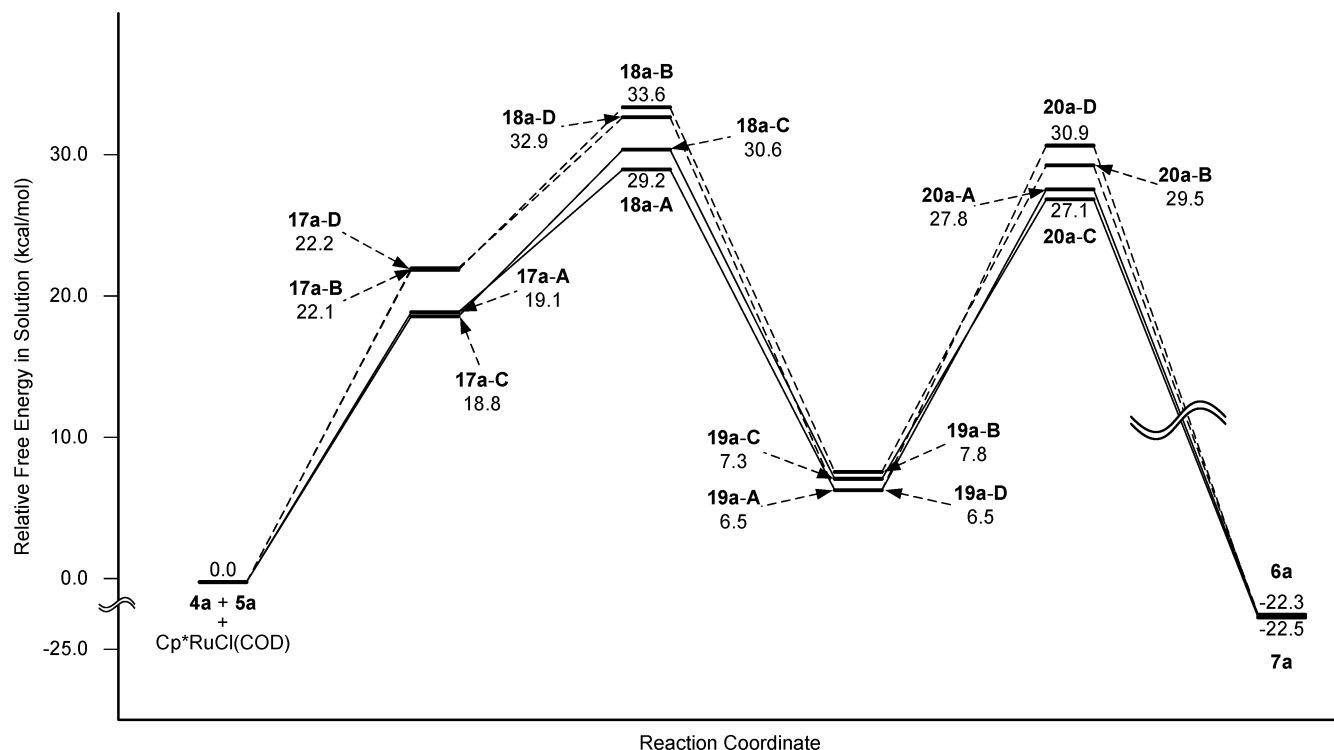


**FIGURE 4.** Potential energy profile by the PCM solvation model for Ru-catalyzed [2+2] cycloaddition between norbornene **4a** ( $Y = \text{exo-OAc}$ ) and alkyne **5a** ( $R^1 = \text{Ph}$ ,  $R^2 = \text{COOEt}$ ). Energies are free energies in solution (in kcal/mol), with respect to separated reactants **4a** + **5a** +  $\text{Cp}^*\text{RuCl}(\text{COD})$ . THF ( $\epsilon = 7.58$ ) was used as solvent in the PCM calculations.

C are preferred, leading to product **7**. Compared to the gas-phase results for  $\Delta\Delta G_{298}^\ddagger(\text{theory})$  in Table 4, the free energies in solution have a smaller mean absolute error, 0.22 kcal/mol. For entries 3 and 8 that showed a greater deviation from experiment in the gas-phase calculations, selectivities predicted in solution are in better agreement with the experimental results. In the solvation model, entries 4 and 5 have the greatest deviation from experiment results, 0.6 and 0.5 kcal/mol, respectively. (Thus, similar trends in the predicted regioselectivities can be observed in the PCM model, in the gas phase, and in the experiments.)

Natural population analyses (NPA)<sup>19b,c</sup> on the rate-determining transition-state structures **18a** were carried out to study the electronic effects of the remote substituents. The NPA charges with hydrogens summed into the heavy atoms on  $\text{C}^5$ ,  $\text{C}^6$ ,  $\text{C}^a$ , and  $\text{C}^b$  in structures **18a-A** to **18a-D** are given in Table 6. Because of the electron-withdrawing ability of COOEt, for all four structures,  $\text{C}^b$ , which is connected to COOEt, is more negatively charged than  $\text{C}^a$ .<sup>20</sup> Because of the inductive effect of the ruthenium, for **18a-A** and **18a-D** where the ruthenium is

**TABLE 6.** NPA Charges with Hydrogens Summed into the Heavy Atoms for  $\text{C}^5$ ,  $\text{C}^6$ ,  $\text{C}^a$ , and  $\text{C}^b$  in Structures **18a-A** to **18a-D**

structure	$\text{C}^5$	$\text{C}^6$	$\text{C}^a$	$\text{C}^b$
<b>18a-A</b>	0.071	-0.022	0.059	-0.202
<b>18a-B</b>	-0.028	0.014	-0.003	-0.132
<b>18a-C</b>	-0.019	0.065	0.052	-0.193
<b>18a-D</b>	0.019	-0.031	-0.009	-0.128

(19) (a) Glendening, E. D.; Reed, A. E.; Carpenter, J. E.; Weinhold, F. *NBO*, version 3.1. (b) Reed, A. E.; Weinhold, F. *J. Chem. Phys.* **1983**, *78*, 4066. (c) Reed, A. E.; Weinstock, R. B.; Weinhold, F. *J. Chem. Phys.* **1985**, *83*, 735.

(20) It should be noted that the polarization of the  $\text{C}^a\text{--C}^b$  bond is also important for the regioselectivity. If  $\text{C}^a$  and  $\text{C}^b$  are both connected to electron-donating groups, such as in the alkyne **4g** ( $R^1 = \text{Ph}$ ,  $R^2 = \text{CH}_3$ ), the  $\text{C}^a$  and  $\text{C}^b$  will have similar electrostatic properties. In this case, if there is no obvious steric repulsions or through-space interactions between the substituent  $R^1$  or  $R^2$  and the catalyst, or in other words, if the orientation of the alkyne does not obviously affect the stability of the transition state **18**, the activation energies for **18-A** and **18-D** (or **18-B** and **18-C**) should be similar. Thus, no obvious regioselectivity could exist. However, interactions between substituents on the alkyne and the catalyst might be masked. Theoretical studies of the effects of different alkynes on reactivity and selectivity will need to be pursued.

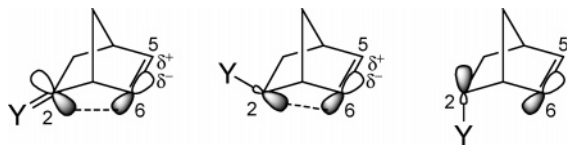
adjacent to  $\text{C}^6$ ,  $\text{C}^6$  is more negative than  $\text{C}^5$ , and for **18a-B** and **18a-C** where ruthenium is adjacent to  $\text{C}^5$ ,  $\text{C}^6$  is more positive than  $\text{C}^5$ . In the transition state **18a-A** in which the  $\text{C}^5\text{--C}^b$  bond is forming,  $\text{C}^5$  is positive and  $\text{C}^b$  is negative. Thus, **18a-A** is stabilized by the electrostatic attraction. In the transition state **18a-B** in which the  $\text{C}^6\text{--C}^a$  bond is forming,  $\text{C}^6$  is positive and  $\text{C}^a$  is nearly neutral. Thus, there is no such electrostatic stabilization in **18a-B**. For the other two transition states, **18a-C** benefits from this electrostatic stabilization and **18a-D** does not. Thus, considering the orientation of the alkynes, pathways **A** and **C**, in which the electron-donating phenyl group is adjacent to ruthenium, are favored. With the same orientation of alkynes,



**TABLE 7.** Selected Bond Lengths (Å) and Percentage Changes from Unsubstituted Norbornene **4n**, Wiberg Indices, and Orbital Interactions (kcal/mol) for Norbornenes with Different 2-Substituents

entry	norbornene	Y	$r(\text{C}^2\text{--C}^6)$ ( $\Delta r$ %)	$r(\text{C}^3\text{--C}^5)$ ( $\Delta r$ %)	WI( $\text{C}^2\text{--C}^6$ )	WI( $\text{C}^3\text{--C}^5$ )	orbital interaction
1	<b>4k</b>	O	2.407 (−2.7)	2.466 (−0.3)	0.0288	0.0101	3.40 <sup>a</sup>
2	<b>4m</b>	C(CN) <sub>2</sub>	2.393 (−3.3)	2.472 (−0.1)	0.0338	0.0088	2.98 <sup>a</sup>
3	<b>4a</b>	exo-OAc	2.455 (−0.8)	2.472 (−0.1)	0.0142	0.0100	1.98 <sup>b</sup>
4	<b>4d</b>	exo-OH	2.476 (+0.1)	2.471 (−0.1)	0.0123	0.0103	1.59 <sup>b</sup>
5	<b>4f</b>	endo-OAc	2.480 (+0.2)	2.473 (−0.0)	0.0109	0.0108	0.62 <sup>c</sup>
6	<b>4i</b>	endo-OH	2.483 (+0.4)	2.470 (−0.2)	0.0107	0.0110	0.74 <sup>c</sup>
7	<b>4n</b>	H	2.474 (0)	2.474 (0)	0.0112	0.0112	0.88 <sup>c</sup>

<sup>a</sup>  $\pi(\text{C}^5\text{--C}^6) \rightarrow \pi^*(\text{C}^2\text{--Y})$  orbital interaction. <sup>b</sup>  $\pi(\text{C}^5\text{--C}^6) \rightarrow \sigma^*(\text{C}^2\text{--Y})$  orbital interaction. <sup>c</sup>  $\pi(\text{C}^5\text{--C}^6) \rightarrow \sigma^*(\text{C}^2\text{--H})$  orbital interaction.

**FIGURE 5.** Orbital interactions between C<sup>2</sup> and C<sup>6</sup>.

the energy and charge distribution differences between pathways **A** and **C** are due solely to the orientations of the norbornenes. In pathway **A**, the C<sup>5</sup>–C<sup>b</sup> bond is formed. In pathway **C**, the C<sup>6</sup>–C<sup>b</sup> bond is formed. C<sup>5</sup> in pathway **A** is slightly more positive than C<sup>6</sup> in pathway **C**. Thus, pathway **A** is slightly favored over pathway **C**.

Having analyzed electron densities and their effects on the stability of the rate-determining transition states **18** on different pathways, two questions are: (i) How does the 2-substituent affect the electronegativities at C<sup>6</sup>? (ii) Why do exo, endo, and unsaturated C-2 substituents show different levels of effect? The electronic effects of the 2-substituent on C<sup>6</sup> can be rationalized by a homoconjugation model. The bent geometry of the bicyclic frameworks orients the orbitals in such a manner that through-space interactions are feasible (Figure 5). For the norbornenes with exocyclic double bonds, **4k** and **4m**, there is homoconjugation between the  $\pi^*(\text{C}^2\text{--Y})$  bond and the  $\pi(\text{C}^5\text{--C}^6)$  bond. For norbornenes with exo-2-substituents, there is homoconjugation between the  $\sigma^*(\text{C}^2\text{--Y})$  bond and the  $\pi(\text{C}^5\text{--C}^6)$  bond. For norbornenes with endo-2-substituents, no strong homoconjugation could exist. The bond distance changes in  $r(\text{C}^2\text{--C}^6)$  of the different 2-substituted norbornenes with respect to norbornene **4n** are shown in Table 7. The distances between C<sup>2</sup>–C<sup>6</sup> decrease ca. 3% for norbornenes with an exocyclic double bond (entries 1 and 2). These shorter distances suggest stronger orbital interactions. The C<sup>2</sup>–C<sup>6</sup> distances of exo-substituted norbornenes (entries 3 and 4) are slightly shorter than those of endo-substituted norbornenes (entries 5 and 6). C<sup>2</sup>–C<sup>6</sup> distances of endo-substituted norbornenes (entries 5 and 6) are slightly longer than that of norbornene itself (entry 7). C<sup>3</sup>–C<sup>5</sup> distances of all substituted norbornenes are quite similar to that of norbornene itself.

More information about orbital interactions of norbornenes with different substituents was obtained using natural bond orbital (NBO) analysis.<sup>19</sup> Wiberg bond indices<sup>21</sup> and orbital interaction energies from NBO analyses are shown in Table 7. The Wiberg index (WI) is usually considered as the order of the corresponding bond in the molecule. It is more sensitive to a change in the bond order than in the bond distance. Entries 1 and 2 in Table 7 have the largest Wiberg indices for C<sup>2</sup>–C<sup>6</sup>, which means the strongest interaction between C<sup>2</sup> and C<sup>6</sup> in

these two structures. Wiberg indices in exo 2-substituted norbornenes (entries 3 and 4) are slightly larger than those in endo 2-substituted norbornenes (entries 5 and 6) and in norbornene itself (entry 7). The Wiberg indices of endo 2-substituted norbornenes (entries 5 and 6) are quite similar to norbornene (entry 7). Norbornenes with different substituents show similar Wiberg indices for C<sup>3</sup>–C<sup>5</sup>.

The interactions between the filled  $\pi(\text{C}^5\text{--C}^6)$  orbital and the empty  $\pi^*(\text{C}^2\text{--Y})$  or  $\sigma^*(\text{C}^2\text{--Y})$  orbital lead to loss of electron density from the donor orbital, the  $\pi(\text{C}^5\text{--C}^6)$  orbital, into the acceptor orbital,  $\pi^*(\text{C}^2\text{--Y})$  or  $\sigma^*(\text{C}^2\text{--Y})$ . The strength of these interactions can be used as a measure of delocalization.<sup>22</sup> The  $\pi(\text{C}^5\text{--C}^6) \rightarrow \pi^*(\text{C}^2\text{--Y})$  interaction is 3.40 kcal/mol for **4k** (Table 7, entry 1) and 2.98 kcal/mol for **4m** (Table 7, entry 2). The  $\pi(\text{C}^5\text{--C}^6) \rightarrow \sigma^*(\text{C}^2\text{--Y})$  interaction is smaller than the  $\pi \rightarrow \pi^*$  interaction and is 1.98 kcal/mol for **4a** (Table 7, entry 3) and 1.59 kcal/mol for **4d** (Table 7, entry 4). For endo 2-substituted norbornenes, no  $\pi(\text{C}^5\text{--C}^6) \rightarrow \sigma^*(\text{C}^2\text{--Y})$  interactions were observed in the computed results. For the exo-H at the C-2 position, the  $\pi(\text{C}^5\text{--C}^6) \rightarrow \sigma^*(\text{C}^2\text{--H})$  interaction is smaller than 1 kcal/mol (Table 7, entries 5–7).

In conclusion, bond lengths, Wiberg indices, and orbital interaction analyses all suggest that the norbornenes with an exocyclic double bond (Table 7, entries 1 and 2) have the greatest degree of homoconjugation. Norbornenes with exo-2-substituents (Table 7, entries 3 and 4) have weaker homoconjugation than those with an exocyclic double bond. No homoconjugation could be observed for the norbornenes with endo-2-substituents (Table 7, entries 5 and 6). The homoconjugations led to electron delocalization from the  $\pi(\text{C}^5\text{--C}^6)$  orbital into the  $\pi^*(\text{C}^2\text{--Y})$  orbital or the  $\sigma^*(\text{C}^2\text{--Y})$  orbital. Thus, the C<sup>5</sup>–C<sup>6</sup> is polarized. C<sup>5</sup> has a more positive charge than C<sup>6</sup> (Figure 5). A greater degree of delocalization leads to a greater C<sup>5</sup>–C<sup>6</sup> polarization. C<sup>5</sup> will be more negative, and C<sup>6</sup> will be more positive.

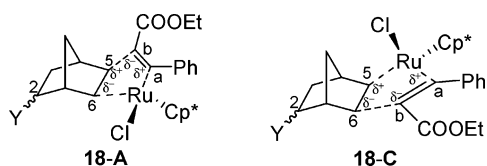
To study the effect of orbital interactions and C<sup>5</sup>–C<sup>6</sup> polarizations on the oxidative addition transition state **18**, Mulliken population analyses were carried out for C<sup>5</sup> and C<sup>6</sup> of **18-A** and **18-C** (Table 8). The charges and the changes in the charges relative to the unsubstituted transition states are given in Table 8. The changes in the charges at C<sup>5</sup> for the substituted relative to the unsubstituted transition states are not large (less than 0.010 electrons, except for entries 6–8 for **18-C**). Greater distances from the C<sup>2</sup> substituents may have caused the smaller changes. For C<sup>6</sup>, the changes in the charges are in agreement with the discussion above. For endo-substituents (entries 1 and 2) where no obvious orbital interactions exist,

(22) (a) Weinhold, F. *Nature* **2001**, *411*, 539. (b) Schreiner, P. R. *Angew. Chem., Int. Ed.* **2002**, *41*, 3579. (c) Pophristic, V.; Goodman, L. *Nature* **2001**, *411*, 565.

(21) Wiberg, K. B. *Tetrahedron* **1958**, *24*, 1083.

**TABLE 8.** Mulliken Charges and Changes in These Charges Relative to the Transition State Structures of the Parent Norbornene (entry 9) for C<sup>5</sup> and C<sup>6</sup> in **18-A** and **18-C**

entry	norbornene	Y	alkyne	R <sup>1</sup>	R <sup>2</sup>	18-A		18-C	
						C <sup>5</sup>	C <sup>6</sup>	C <sup>5</sup>	C <sup>6</sup>
1	<b>4f</b>	<i>endo</i> -OAc	<b>5a</b>	Ph	COOEt	-0.099 (-0.002)	-0.155 (-0.004)	-0.154 (-0.003)	-0.103 (-0.006)
2	<b>4i</b>	<i>endo</i> -OH	<b>5a</b>	Ph	COOEt	-0.100 (-0.003)	-0.145 (+0.006)	-0.150 (+0.001)	-0.086 (+0.011)
3	<b>4d</b>	<i>exo</i> -OH	<b>5a</b>	Ph	COOEt	-0.098 (-0.001)	-0.163 (-0.012)	-0.154 (-0.003)	-0.110 (-0.013)
4	<b>4a</b>	<i>exo</i> -OAc	<b>5a</b>	Ph	COOEt	-0.100 (-0.003)	-0.169 (-0.018)	-0.160 (-0.009)	-0.115 (-0.018)
5	<b>4k</b>	O	<b>5a</b>	Ph	COOEt	-0.095 (+0.002)	-0.185 (-0.034)	-0.159 (-0.008)	-0.117 (-0.020)
6	<b>4k</b>	O	<b>5b</b>	<sup>n</sup> Bu	COOEt	-0.095 (+0.002)	-0.198 (-0.047)	-0.171 (-0.020)	-0.118 (-0.021)
7	<b>4k</b>	O	<b>5c</b>	Cy	COOEt	-0.108 (-0.011)	-0.197 (-0.046)	-0.170 (-0.019)	-0.129 (-0.032)
8	<b>4m</b>	C(CN) <sub>2</sub>	<b>5c</b>	Cy	COOEt	-0.107 (-0.010)	-0.189 (-0.038)	-0.166 (-0.015)	-0.132 (-0.035)
9	<b>4</b>	H	<b>5a</b>	Ph	COOEt	-0.097 (0)	-0.151 (0)	-0.151 (0)	-0.097 (0)

**FIGURE 6.** The orbital interactions give a more positive charge to C<sup>5</sup> and a more negative charge to C<sup>6</sup>. This will stabilize **18-A** and destabilize **18-C** because of the electrostatic interactions.

the charges on C<sup>6</sup> are about the same as those in the unsubstituted transition states (entry 9). For *exo*-substituents (entries 3 and 4) where weak orbital interactions exist, the charges for C<sup>6</sup> are slightly more negative (0.010–0.020 electrons) than those in the unsubstituted transition states. For the substituents with an exocyclic double bond (entries 5–8) where greater orbital interactions exist, the charges for C<sup>6</sup> are much more negative (0.020–0.050) than those for the unsubstituted transition states. These changes in the charges in particular may be viewed in light of the homoconjugation model discussed above (Figure 5).

The Mulliken charge analyses suggest that the orbital interactions in the substituted norbornenes will also affect the C<sup>5</sup>–C<sup>6</sup> bond polarization of the oxidative addition transition state **18**. A stronger orbital interaction will lead to a more negative C<sup>6</sup>. For the transition states **18-C** in which C<sup>6</sup> is forming a bond with the negatively charged C<sup>b</sup>, a more negative C<sup>6</sup> will destabilize the transition state. In **18-A**, this destabilization does not exist (Figure 6). Thus, a stronger orbital interaction will increase the activation energy difference between pathways A and C and finally leads to a greater regioselectivity.

## Conclusion

In conclusion, we have demonstrated the first examples of the remote substituent effect on the regioselectivity of ruthenium-catalyzed [2+2] cycloadditions between 2-substituted norbornenes and unsymmetrical alkynes. Most of the cycloadditions occurred smoothly at room temperature, giving the cycloadducts in excellent yields (usually above 90% except for less reactive alkynes **5e** and **5f**). Regioselectivities of 1.2:1 to 15:1 were observed with various substituents at the C-2 position of norbornenes. *Exo*-2-substituents usually showed a greater remote substituent effect on the regioselectivity of the cycloaddition than the corresponding *endo*-2-substituents (Table 1 vs Table 2). The regioselectivity of the cycloadditions with the C-2 substituents containing an exocyclic double bond (sp<sup>2</sup>-hybridized carbon at C<sup>2</sup>) is much higher than that of the cycloadditions with the *exo*- and *endo*-2-substituted norbornenes (Table 3 and Scheme 4 vs Tables 1 and 2). These studies on the remote

substituent effects observed in the ruthenium-catalyzed [2+2] cycloadditions are significant because such a high level of remote substituent effect is seldom observed in any transition-metal-catalyzed cycloaddition reactions.

Theory predicted the same trends as experiment and matched the experimental product ratios well. The different regioselectivities were interpreted by comparison of activation energies, stereoelectronic analysis, and orbital interactions.  $\pi(C^5-C^6) \rightarrow \pi^*(C^2-Y)$  is the strongest orbital interaction which exists in the norbornenes containing an exocyclic double bond.  $\pi(C^5-C^6) \rightarrow \sigma^*(C^2-Y)$  is a weaker interaction which exists in the *exo*-2-substituted norbornenes. The *endo*-2-substituted norbornenes do not have such orbital interactions. A stronger orbital interaction will not only change the geometric and electrostatic properties of the 2-substituted norbornene reactants but also increase the degree of C<sup>5</sup>–C<sup>6</sup> bond polarization in the rate-determining transition-state structure **18**. This bond polarization gives C<sup>6</sup> a more negative charge at transition state **18**, which is not favorable to bond formation between C<sup>6</sup> and the negatively charged C<sup>b</sup> in **18-C**, the transition state leading to the minor isomeric product. A stronger destabilization of **18-C** will increase the difference of activation energies between the two pathways leading to the major and minor isomeric products and finally will result in higher regioselectivity.

## Experimental Section

Only representative procedures and characterizations of the products are described here. Full details can be found in the Supporting Information.

**General Procedure for Ruthenium-Catalyzed [2+2] Cycloadditions.** A mixture of a 2-substituted norbornene (**4a–k**, **4m**) (1.0 mmol, 5 equiv), an alkyne (**5a–g**) (0.2 mmol, 1 equiv), and THF (0.25 mL) in an oven-dried vial was added via a cannula to an oven-dried screw-cap vial containing Cp\*RuCl(COD) (weighed out from a drybox, 0.01 mmol, 5 mol %) under nitrogen. The reaction mixture was stirred in the dark at 25–80 °C for 45–165 h. The crude product was purified by column chromatography (EtOAc–hexane mixtures) to give the cycloadduct.

**Cycloadducts 6a and 7a** (Table 1, entry 1, Y = OAc). Yield: 94% (white solid, **6a/7a** = 4:1 measured by GC and <sup>1</sup>H NMR). *R*<sub>f</sub> = 0.39 (EtOAc/hexanes = 1:9). GC (HP-1 column): retention time for major isomer **6a** = 30.571 min, and retention time for minor isomer **7a** = 30.695 min. IR (CH<sub>2</sub>Cl<sub>2</sub>)  $\nu_{\max}$  (cm<sup>-1</sup>) 3066, 2937, 2969, 1734, 1704, 1617, 1492, 1448, 1374, 1297, 1244, 1217, 1204, 1136, 1109. <sup>1</sup>H NMR (CDCl<sub>3</sub>, 400 MHz)  $\delta$  8.02 (m, 2H), 7.36 (m, 3H), 4.65 (dm, 1H, *J* = 4.6 Hz), 4.23 (q, 2H, *J* = 7.1 Hz), 2.81 (d, 0.8H, *J* = 3.3 Hz), 2.75 (d, 0.2H, *J* = 3.3 Hz), 2.69 (d, 0.2H, *J* = 3.3 Hz), 2.66 (d, 0.8H, *J* = 3.3 Hz), 2.40 (br. s, 0.2H), 2.34–2.36 (m, 1.8H), 2.02 (s, 3H), 1.75 (dd, 1H, *J* = 13.3, 7.3 Hz), 1.60 (ddd, 1H, *J* = 13.3, 3.9, 2.7 Hz), 1.39 (br. s, 2H), 1.33 (t, 3H, *J* = 7.1 Hz). <sup>13</sup>C NMR (APT, CDCl<sub>3</sub>, 100 MHz) major isomer **6a**:  $\delta$  170.7,

162.7, 154.0, 132.1, 130.1, 128.8(2), 128.3, 76.2, 60.0, 44.6, 41.3, 40.1, 38.2, 33.7, 27.7, 21.2, 14.3. Visible peaks for minor isomer **7a**:  $\delta$  170.6, 155.6, 132.2, 127.0, 72.3, 45.0, 41.3, 40.8, 39.7, 38.6, 34.0, 27.8.

Fractional recrystallization of the above mixture in EtOAc/hexanes (1:9) afforded a pure sample of **6a** as white crystals. The regiochemistry of **6a** was determined by NMR experiments ( $^1\text{H}$  NMR, APT, HCOSEY, HSQC, HMBC, and NOESY or GOESY experiments) and confirmed by X-ray crystallography.  $R_f = 0.39$  (EtOAc/hexanes = 1:9). Mp 71 °C. GC (HP-1 column): retention time for major isomer **6a** = 30.571 min. IR ( $\text{CH}_2\text{Cl}_2$ )  $\nu_{\text{max}}$  ( $\text{cm}^{-1}$ ) 3066, 2969, 2937, 1734, 1704, 1617, 1492, 1448, 1374, 1297, 1244, 1217, 1204, 1136, 1109.  $^1\text{H}$  NMR ( $\text{CDCl}_3$ , 400 MHz)  $\delta$  8.02 (m, 2H), 7.31 (m, 3H), 4.63 (dm, 1H,  $J = 5.3$  Hz), 4.22 (q, 2H,  $J = 7.1$  Hz), 2.79 (d, 1H,  $J = 3.3$  Hz), 2.64 (d, 1H,  $J = 3.3$  Hz), 2.35 (br. s, 1H), 2.33 (d, 1H,  $J = 4.0$  Hz), 2.00 (s, 3H), 1.73 (dd, 1H,  $J = 13.3$ , 7.3 Hz), 1.58 (ddd, 1H,  $J = 13.3$ , 3.9, 2.7 Hz), 1.37 (br. s, 2H), 1.31 (t, 3H,  $J = 7.1$  Hz).  $^{13}\text{C}$  NMR (APT,  $\text{CDCl}_3$ , 100 MHz)  $\delta$  170.5, 162.5, 153.9, 132.0, 130.0, 128.7, 128.6, 128.2, 76.1, 59.9, 44.5, 41.2, 40.0, 38.1, 33.6, 27.6, 21.1, 14.2. Anal. Calcd for  $\text{C}_{20}\text{H}_{22}\text{O}_4$ : C, 73.60; H, 6.79. Found C, 73.56; H, 6.77.

**Cycloadducts 11m and 12m** (Scheme 4). Yield: 88% (white solid, **11m/12m** = 15:1 measured by GC and  $^1\text{H}$  NMR).  $R_f = 0.62$  (EtOAc/hexanes = 2:3). GC (HP-1 column): retention time for major isomer **11m** = 20.016 min and for minor isomer **12m** = 20.533 min. IR ( $\text{CH}_2\text{Cl}_2$ )  $\nu_{\text{max}}$  ( $\text{cm}^{-1}$ ) 2985, 2929, 2853, 2233, 1717, 1705, 1699, 1650, 1615, 1450, 1371, 1336, 1267, 1249, 1206, 1185, 1121, 1035.  $^1\text{H}$  NMR ( $\text{CDCl}_3$ , 400 MHz)  $\delta$  4.19 (q, 2H,  $J = 7.1$  Hz), 3.42 (s, 0.06H), 3.33 (s, 0.94H), 2.79 (tt, 1H,  $J = 11.4$ , 3.3 Hz), 2.71 (d, 0.94H,  $J = 3.2$  Hz), 2.65 (dd, 1H,  $J = 19.2$ , 4.4 Hz), 2.63–2.66 (m, 0.12H), 2.55 (m, 1.88H), 2.47 (d, 0.06H), 2.27 (dd, 0.94H,  $J = 19.2$ , 4.2 Hz), 2.25 (dd, 0.06H,  $J = 19.2$ , 4.2 Hz), 1.76 (m, 5H), 1.69 (dm, 1H,  $J = 11.2$  Hz), 1.42 (dm, 1H,  $J = 11.2$  Hz), 1.30 (t, 3H,  $J = 7.1$  Hz), 1.14–1.35 (m, 5H).  $^{13}\text{C}$  NMR (APT,  $\text{CDCl}_3$ , 100 MHz) major isomer **11m**:  $\delta$  190.1, 163.8, 162.1, 129.8, 111.5, 111.4, 80.3, 60.1, 45.6, 43.2, 42.5, 39.1, 38.8, 33.7, 31.7, 30.7, 30.3, 25.8, 25.60, 25.57, 14.3. Visible peaks for minor isomer **12m**:  $\delta$  45.4, 44.6, 41.5, 39.3, 34.1.

The major isomer **11m** was isolated from the above mixture using a Chromatotron (EtOAc/hexanes = 1:9, 1:4) as a white solid. The regiochemistry of **11m** was characterized through the use of NMR experiments ( $^1\text{H}$  NMR, APT, HSQC, and NOESY) and confirmed by X-ray crystallography. Mp 88–89 °C. GC (HP-1 column): retention time = 19.921 min.  $^1\text{H}$  NMR ( $\text{CDCl}_3$ , 400 MHz)  $\delta$  4.19 (q, 2H,  $J = 7.1$  Hz), 3.33 (s, 1H), 2.79 (tm, 1H,  $J = 11.2$  Hz), 2.71 (d, 1H,  $J = 3.1$  Hz), 2.65 (dd, 1H,  $J = 19.2$ , 4.4 Hz), 2.55 (m, 2H), 2.27 (dd, 1H,  $J = 19.2$ , 4.2 Hz), 1.68–1.78 (m, 6H), 1.42 (dm, 1H,  $J = 11.2$  Hz), 1.30 (t, 3H,  $J = 7.1$  Hz), 1.19–1.32 (m, 5H).  $^1\text{H}$  NMR ( $\text{C}_6\text{D}_6$ , 400 MHz)  $\delta$  3.96 (q, 2H,  $J = 7.1$  Hz), 2.83 (s, 1H), 2.73 (tt, 1H,  $J = 11.6$ , 3.2 Hz), 2.16 (d, 1H,  $J = 3.1$  Hz), 1.96 (d, 1H,  $J = 4.0$  Hz), 1.84 (d, 1H,  $J = 3.1$  Hz), 1.72 (ddd, 1H,  $J = 19.1$ , 4.0, 0.9 Hz), 1.50–1.61 (m, 5H), 1.47 (dd, 1H,  $J = 19.1$ , 4.1 Hz), 1.22 (ddm, 1H,  $J = 11.1$ , 4.1 Hz), 1.03–1.13 (m, 3H), 0.91–1.01 (m, 2H), 0.94 (t, 3H,  $J = 7.1$  Hz), 0.53 (dd, 1H,  $J = 11.1$ , 0.9 Hz).  $^{13}\text{C}$  NMR (APT,  $\text{CDCl}_3$ , 100 MHz)  $\delta$  190.1, 163.9, 162.1, 129.8, 111.53, 111.45, 80.4, 60.1, 45.6, 43.3, 42.5, 39.1, 38.8, 33.7, 31.7, 30.7, 30.3, 25.8, 25.61, 25.58, 14.3. Anal. Calcd for  $\text{C}_{21}\text{H}_{24}\text{O}_2\text{N}_2$ : C, 74.97; H, 7.19. Found C, 74.87; H, 7.15.

## Computational Details

All computations in this study were carried out with the Gaussian 98<sup>23</sup> suite of programs. The Becke three-parameter hybrid functional<sup>24</sup> combined with the Lee, Yang, and Parr (LYP) correlation functional,<sup>25</sup> B3LYP, was used. The Los Alamos effective core potential plus double- $\zeta$  basis set LANL2DZ<sup>26</sup> was employed on ruthenium, and the 6-31G(d) basis set<sup>27</sup> was used for the rest of the atoms. All electronic structures were closed shells. Harmonic vibrational frequencies were computed to verify the nature of the stationary points. Transition-state structures were characterized by one imaginary frequency and are first-order saddle points. To ensure that the transition states link the products to the expected reactants, the normal modes corresponding to the imaginary frequencies were animated. All reactant and product structures exhibited zero imaginary frequencies and are minima. The relative Gibbs free energies ( $\Delta G$  values) were obtained by taking into account zero-point energies, thermal motion, and entropy contribution at standard conditions (temperature of 298 K, pressure of 1 atm). Natural bond orbital (NBO) analyses were performed with the NBO program<sup>19</sup> in Gaussian 98. The resulting natural population analysis (NPA) charge,<sup>19b,c</sup> Wiberg indices,<sup>21</sup> and orbital interactions<sup>22</sup> were used for a detailed study of the electronic structure and bond interactions. The solvation energies,  $G_{298}(\text{THF})$ , were computed using the polarized continuum model of Tomasi and co-workers<sup>18</sup> as implemented in Gaussian 98. THF ( $\epsilon = 7.58$ ), which was used in the experiments, is specified as the solvent in the solvation model.

**Acknowledgment.** This work was supported by NSERC (Canada) and Boehringer Ingelheim (Canada). W.T. thanks Boehringer Ingelheim (Canada) Ltd. for a Young Investigator Award, and R.W.J. thanks the Ontario government and NSERC (Canada) for postgraduate scholarships (OGS and NSERC PGS B).

**Supporting Information Available:** Detailed experimental procedures, full characterization of new compounds, and listing of Cartesian coordinates and total energies for the optimized geometries of calculated species. This material is available free of charge via the Internet at <http://pubs.acs.org>.

JO060103L

(23) Frisch, M. J.; Trucks, G. W.; Schlegel, H. B.; Scuseria, G. E.; Robb, M. A.; Cheeseman, J. R.; Zakrzewski, V. G.; Montgomery, J. A., Jr.; Stratmann, R. E.; Burant, J. C.; Dapprich, S.; Millam, J. M.; Daniels, A. D.; Kudin, K. N.; Strain, M. C.; Farkas, O.; Tomasi, J.; Barone, V.; Cossi, M.; Cammi, R.; Mennucci, B.; Pomelli, C.; Adamo, C.; Clifford, S.; Ochterski, J.; Petersson, G. A.; Ayala, P. Y.; Cui, Q.; Morokuma, K.; Salvador, P.; Dannenberg, J. J.; Malick, D. K.; Rabuck, A. D.; Raghavachari, K.; Foresman, J. B.; Cioslowski, J.; Ortiz, J. V.; Baboul, A. G.; Stefanov, B. B.; Liu, G.; Liashenko, A.; Piskorz, P.; Komaromi, I.; Gomperts, R.; Martin, R. L.; Fox, D. J.; Keith, T.; Al-Laham, M. A.; Peng, C. Y.; Nanayakkara, A.; Challacombe, M.; Gill, P. M. W.; Johnson, B.; Chen, W.; Wong, M. W.; Andres, J. L.; Gonzalez, C.; Head-Gordon, M.; Replogle, E. S.; Pople, J. A. *Gaussian 98*, revision A.11; Gaussian, Inc.: Pittsburgh, PA, 2001.

(24) Becke, A. D. *J. Chem. Phys.* **1993**, *98*, 5648.

(25) Lee, C.; Yang, W.; Parr, R. G. *Phys. Rev. B* **1988**, *37*, 785.

(26) Hay, P. J.; Wadt, W. R. *J. Chem. Phys.* **1985**, *82*, 299.

(27) (a) Ditchfield, R.; Hehre, W. J.; Pople, J. A. *J. Chem. Phys.* **1971**, *54*, 724. (b) Hehre, W. J.; Ditchfield, R.; Pople, J. A. *J. Chem. Phys.* **1972**, *56*, 2257. (c) Hariharan, P. C.; Pople, J. A. *Theor. Chim. Acta* **1973**, *28*, 213. (d) Hariharan, P. C.; Pople, J. A. *Mol. Phys.* **1974**, *27*, 209. (e) Gordon, M. S. *Chem. Phys. Lett.* **1980**, *76*, 163.